Supplementary Information (SI) for Journal of Materials Chemistry A.

Supporting information for:

Efficient photocatalytic nitrogen reduction of MoS_2 doped with transition metal and sulfur-containing vacancies: enhanced nitrogen activation and inhibition of water decomposition

Qiang Fu[a], Zhiling Huang[b], Zheming Ni[a], Shengjie Xia[a]*

[a] *Department of Chemistry, College of Chemical Engineering, Zhejiang University of Technology, 18 Chaowang Road, Hangzhou 310014, P R China*

[b] *Department of Pharmaceutical Engineering, School of Life and Health Sciences, Huzhou College, Huzhou 313000, P. R. China*

---

* Corresponding author.

E–mail: xiasj@zjut.edu.cn (S.J. Xia)

Telephone number: 086–0571–88320373

1. Characterization of catalysts

The instrument model used for XRD testing in this paper is Empyrean, using Cu-K α radiation source, radiation wavelength λ= 0.1541 nm, tube voltage of 45 kV, tube current of 40 mA, testing angle of 10~80 °.

The method of SEM scanning catalysts is to excite various information through high-energy electron beams, the interaction between the beam and the catalyst, and collect, amplify, and re image to characterize the microstructure of the catalyst. The scanning electron microscope used in this paper is Gemini (Zeiss, Germany).

TEM is a microscope that uses the wavelength and square root of the voltage of an electron beam to alter the atomic collisions in a catalyst, resulting in stereo angular scattering. It is used to observe the fine structure of the sample. The model of the transmission electron microscope used in this paper is Tecnai G2 F30.

UV visible diffuse reflectance spectroscopy mainly uses the reflection of light on the surface of a substance to obtain information about the catalyst, and is used to study the light absorption capacity and bandgap of the catalyst. This paper uses the Shimadzu UV-2600 UV visible spectrophotometer from Japan, with $BaSO_4$ as the background, to scan at 200-800 nm.

An X-ray photoelectron spectrometer (XPS. Thermo Scientific K-Alpha) was used to characterize the energy band structure and the chemical state of the surface elements.

This paper conducted the tests on the electrochemical workstation CHI750E, dispersing 10 mg of powder sample in 1 mL of ultrapure water/ethanol solution, and then adding 50 μL Nafion solution, sonicate for 30 minutes. Drip 100 μL suspension onto ITO glass, air dry at room temperature for photoelectric testing. The testing conditions for transient photocurrent and electrochemical impedance are: turn on the light for 20 seconds, turn off the light for 20 seconds, and repeat more than 4 cycles;

Light source: 300 W xenon lamp; Bottom solution: 0.5 M Na_2SO_4 solution.

2. Photocatalytic ammonia synthesis experiment

2.1 Experimental apparatus for photocatalytic synthesis of ammonia

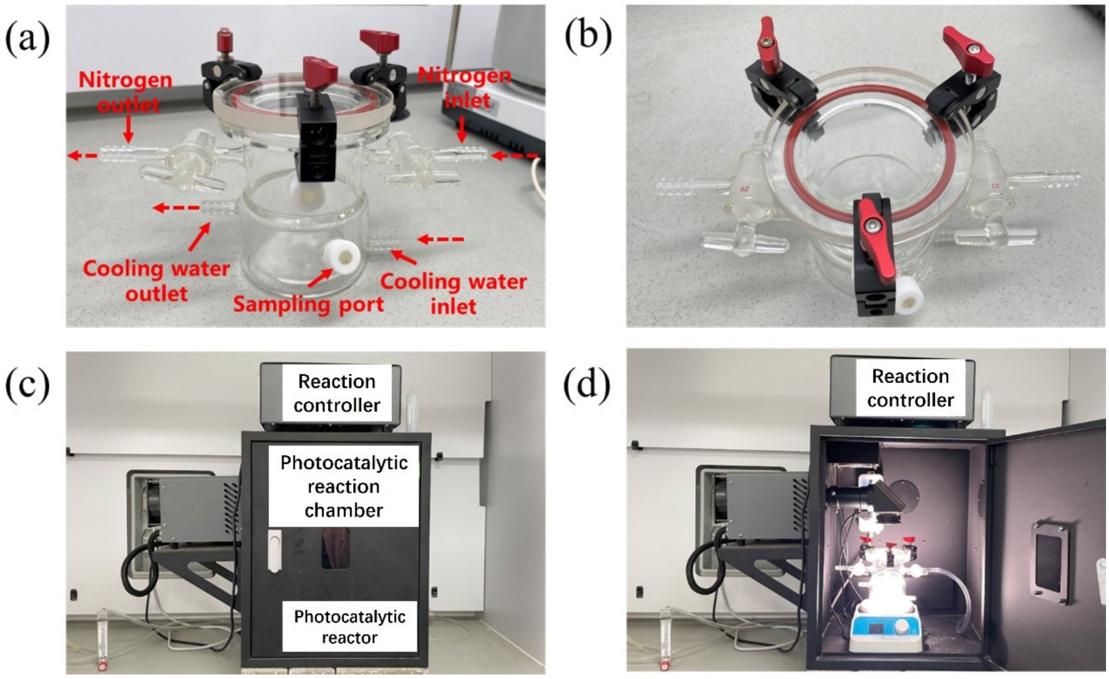

Figure S1. Schematic diagram of Photocatalytic ammonia setup: photocatalytic quartz reactor (a) side view; (b) top view and Xe light sources (c and d)

2.2 Standard curve for photocatalytic synthesis of ammonia

There are three types of detection agents for the salicylic acid method. Detection agent A is a 1 M NaOH solution containing 5 wt% salicylic acid and 5 wt% sodium citrate, detection agent B is a 0.05 M NaClO solution, and detection agent C is a 1 wt% sodium nitroprusside solution.

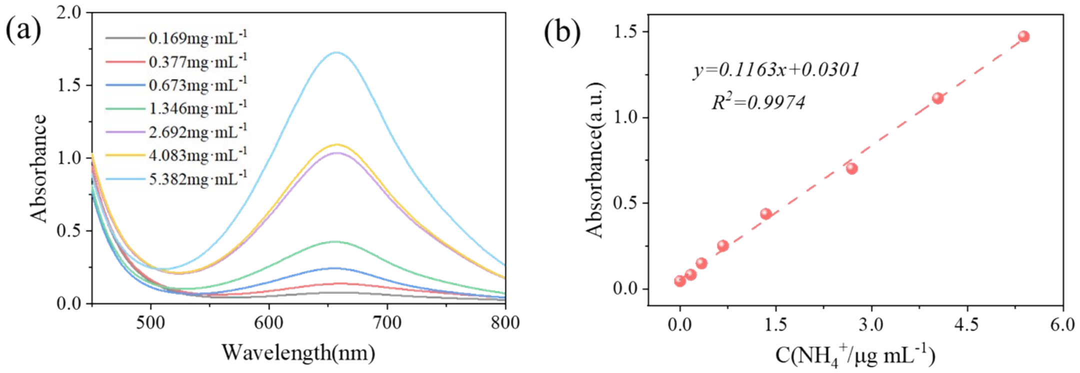

Figure S2. (a) The UV-visible absorption spectrum of NH_4^+; (b) Standard curve of Salicylic acid method for detecting NH_4^+ (C is the concentration, A is the absorbance)

Standard curve configuration: First, weigh 1.0 g of NH_4Cl and dry it in an air drying oven for 2 hours. Then configure NH_4Cl to 4 μg·mL^{-1} ammonia standard solution. Using 1000 μL pipette takes 0, 50, 100, 150, 200, 250, 400, 750, 1250, and 2000 μL NH_4^+ standard solution, respectively, add into 5 mL colorimetric tubes and dilute to 2 mL with distilled water. Finally, add 2 mL of reagent A, 1 mL of reagent B, and 0.2 mL of reagent C to the aforementioned series of solutions, shake well, and let stand for 2 hours. Using a UV visible spectrophotometer to scan at 200-800 nm, the UV visible absorption spectrum was obtained, as shown in **Figure S2a**. And then the standard curve of NH_4^+ absorbance A - concentration C was obtained by linear fitting at λ=655 nm, as shown in **Figure S2b**.

3. Calculation methods and models

All calculations in this work were carried out using the Dmol^3 [1] module of Materials Studio 8.0 software. Using density functional theory (GGA-PBE) combined with generalized gradient approximations and Perdew Burke Ernzerhof functionals [2, 3]. Involving doping of transition metal atoms, the effective nuclear potential (ECP) method is used for inner electrons, and the valence electron wave function is expanded through a dual numerical orbital basis set and orbital polarization function (DNP) [4]. In order to better describe the van der Waals force interaction between small molecule adsorption and surface, the DFT-D3 experience of Grimme method was used for correction [4,5]. The requirements for structural optimization are that the energy difference is less than 1 × 10^{-5} Ha, the convergence of forces on each atom is 0.004 Ha·$Å^{-1}$, the atomic displacement is less than 0.005 Å, and the convergence standard for the self-consistent field (SCF) is 1 × 10^{-5} Ha. Perform geometric optimization using Brillouin zone integration at 2x2x1 K points. Simulate the surface by introducing a 20 Å vacuum layer on the z-axis and avoiding the interaction between two adjacent periodic units. Considering the introduction of individual metal atoms in the material system and the presence of free radical intermediates in the reaction pathway, spin polarization is not restricted during calculation. The electronic properties of the adsorption system were analyzed using density of states (DOS), and the charge distribution and transfer of the adsorption system were analyzed using Mulliken charges [6]. All models have undergone structural optimization and vibration frequency analysis calculations.

To illustrate the adsorption strength of the catalyst on small molecules, the adsorption energy (E_{ads}) of small molecules on the catalyst is calculated using the following formula [7]:

$$E_{ads} = E_{tot} - E_{cat} - E_{mol} \tag{S1}$$

In the formula, E_{tot} represents the total energy of the catalyst after adsorbing small molecules, and E_{mol} represents the energy of the adsorbed small molecules. The negative adsorption energy indicates that an exothermic reaction has occurred and the resulting complex is thermodynamically ideal.

Using Computational Hydrogen Electrodes (CHE) to calculate Gibbs Free Energy changes in electrochemical processes (ΔG) [8], where the chemical potential of one H^+/e^- is equivalent to half of an isolated H_2 molecule, the reaction steps on the catalyst are ΔG is calculated using the following equation [9]:

$$\Delta G = \Delta E + \Delta E_{ZPE} - T\Delta S + \Delta G_U + \Delta G_{pH} \tag{S2}$$

In the formula ΔE represents the energy difference between the optimized reactants and products, ΔE_{ZPE} and S respectively represent the zero-vibration energy and entropy change caused by the reaction, calculated from frequency. T represents the temperature during the reaction, and in the calculation, T is set to the ambient temperature (298.15 K). ΔG_{U} is the contribution of electrode potential U, defined as: $\Delta G_U = - neU$, n is the number of transferred electrons, e and U represent the number of transferred electrons and applied voltage during the reaction process, and U is set to 0 during the calculation process. Besides U, the pH value of the environment also affects ΔG has an impact. According to the definition, $\Delta G_{pH} = - k_B T ln[H^+] = pH \times k_B T \times ln10$, where k_{B} is the Boltzmann constant. In all calculations, pH is set to 0.

To evaluate the stability of MoS_2 structure after constructing S vacancies, the formation energy (E_{f}) was calculated using the following equation [10]:

$$E_f = E_{V_S - MoS_2} + 3E_S - E_{MoS_2} \tag{1}$$

$$E_S = E_{H_2S} - E_{H_2} \tag{2}$$

In the formula, E_{MoS_2} represents the total energy of MoS_2, $E_{V_S - MoS_2}$ represents the total energy of MoS_2 after the formation of S vacancies, E_S represents the energy of S atoms in H_2S, E_{H_2S} and E_{H_2}represent the energy of H_2S and H_2, respectively.

Reference

[1] J.P. Perdew, J.A. Chevary, S.H. Vosko, K.A. Jackson, M.R. Pederson, D.J. Singh, C. Fiolhais, Atoms, molecules, solids, and surfaces: Applications of the generalized gradient approximation for exchange and correlation, Phys. Rev. B, 46 (1992) 6671-6687.

[2] J.P. Perdew, K. Burke, M. Ernzerhof, Generalized gradient approximation made simple, Phys. Rev. Lett., 77 (1996) 3865-3868.

[3] P. Liu, J.A. Rodriguez, Catalysts for hydrogen evolution from the [NiFe] hydrogenase to the $Ni_2P(001)$ surface: The importance of ensemble effect, J. Am. Chem. Soc., 127 (2005) 14871-14878.

[4] S. Grimme, J. Antony, S. Ehrlich, H. Krieg, A consistent and accurate ab initio parametrization of density functional dispersion correction (DFT-D) for the 94 elements H-Pu, J. Chem. Phys., 132 (2010) 154104.

[5] M. Franco-Pérez, J.L. Gázquez, Electronegativities of Pauling and Mulliken in Density Functional Theory, J. Phys. Chem. A, 123 (2019) 10065-10071.

[6] Z.Y. Gao, Y. Meng, H. Shen, B. Xie, Z. Ni, S. Xia, Theoretical study on low temperature reverse water gas shift (RWGS) mechanism on monatomic transition metal M doped C_2N catalyst (M=Cu, Co, Fe), Mol. Catal., 516 (2021) 111992.

[7] A.A. Peterson, F. Abild-Pedersen, F. Studt, J. Rossmeisl, J.K. Nørskov, How copper catalyzes the electroreduction of carbon dioxide into hydrocarbon fuels, Energy Environ. Sci., 3 (2010) 1311-1315.

[8] J.X. Zhao, Z.F. Chen, Single Mo atom supported on defective boron nitride monolayer as an efficient electrocatalyst for nitrogen fixation: A computational study, J. Am. Chem. Soc., 139 (2017) 12480-12487.

[9] Q. Dang, S.B. Tang, T.Y. Liu, X.K. Li, X. Wang, W. Zhong, Y. Luo, J. Jiang, Regulating electronic spin moments of single-atom catalyst sites via single-atom promoter tuning on S-vacancy MoS_2 for efficient nitrogen fixation, J. Phys. Chem. Lett., 12 (2021) 8355-8362.

[10] B. Delley, An all-electron numerical method for solving the local density functional for polyatomic molecules, J. Chem. Phys., 92 (1990) 508-517.

Table S1. Formation energies (E_f) of TM atoms doped at sites 1 and 2 in V_S−MoS_2

Structural	E_f (Site 1) (eV)	E_f (Site 2) (eV)
V_S−MoS_2	–	–
Sc@V_S−MoS_2	1.240	1.418
Cu@V_S−MoS_2	−0.151	0.042
V@V_S−MoS_2	0.971	1.039

Table S2. Information on the composition and elemental content of five samples tested by ICP.

Sample	Sc(wt%)	Cu(wt%)	V(wt%)	Mo(wt%)	S(wt%)
MoS_2	–	–	–	58.2	41.8
V_S-MoS_2	–	–	–	59.3	40.7
Sc@V_S-MoS_2	1.38	–	–	58.75	39.87
Cu@V_S-MoS_2	–	1.42	–	58.98	39.60
V@V_S-MoS_2	–	–	1.45	59.19	39.36

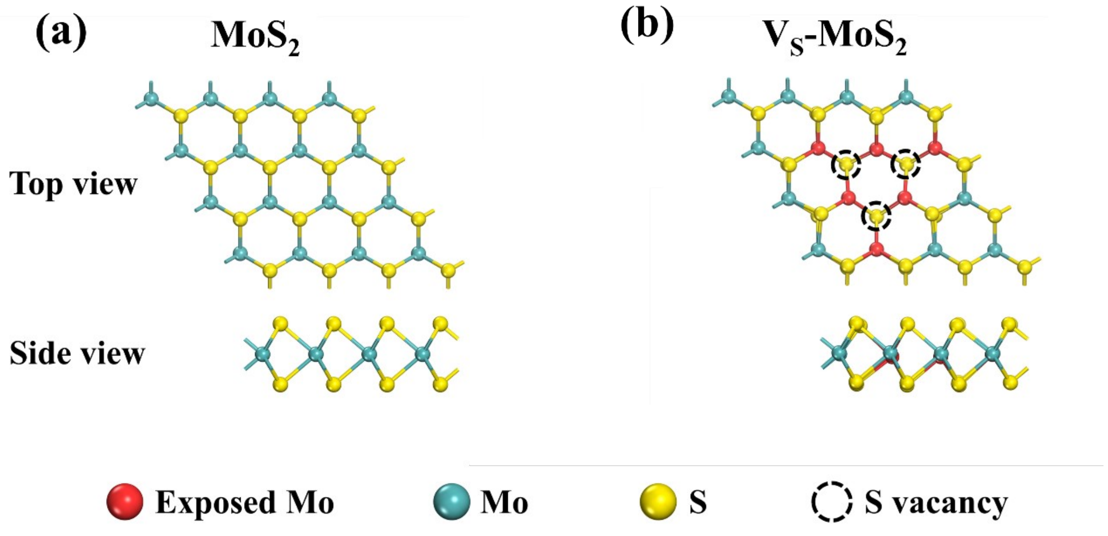

Figure S3. Optimized structural models of (a) MoS_2, (b) V_S−MoS_2.

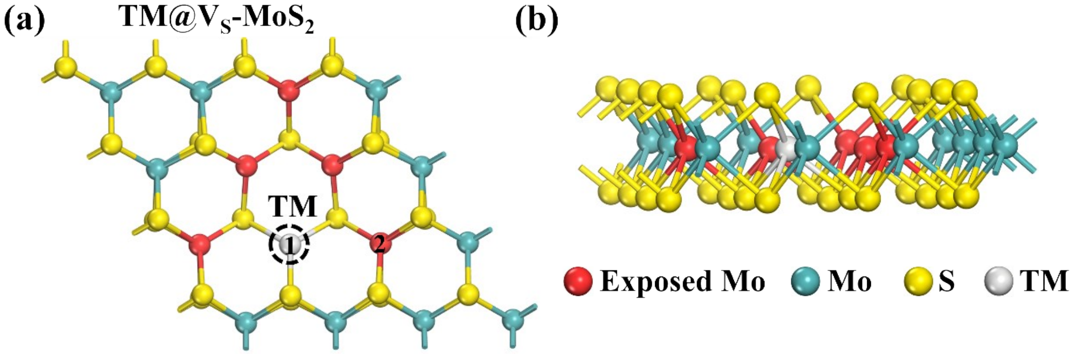

Figure S4. Top view (a) and side view (b) of the structure of TM@V$_S$−MoS$_2$ (1 and 2 are the doping sites of the TM atoms). Note: doping of transition metal (TM) atoms was carried out at sites 1 and 2 on V$_S$-MoS$_2$, and the formation energies of TM atom doped structures were compared.

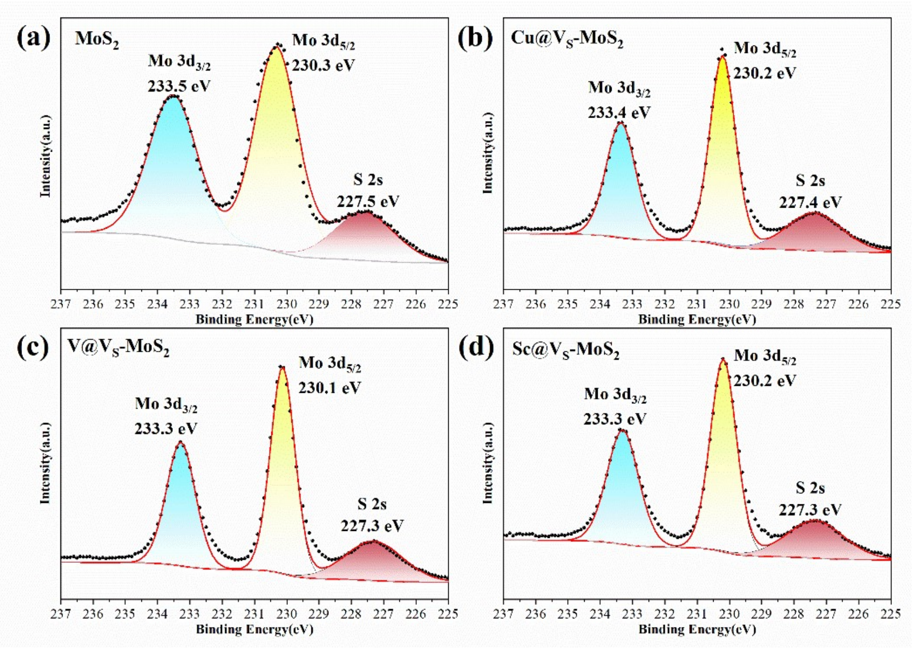

Figure S5. Deconvoluted Mo 3d XPS spectra. (a) Pristine MoS$_2$, (b) Cu-doped MoS$_2$ with sulfur vacancies (Cu@Vs-MoS$_2$), (c) V-doped Vs-MoS$_2$ (V@Vs-MoS$_2$), and (d) Sc-doped Vs-MoS$_2$ (Sc@Vs-MoS$_2$).

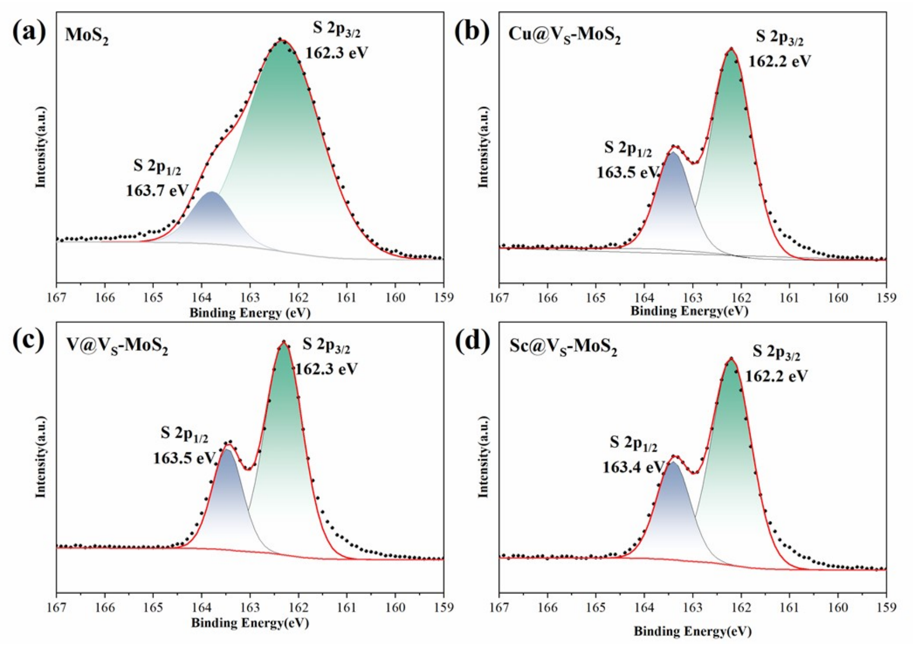

Figure S6. Deconvoluted S 2p XPS spectra. (a) Pristine MoS_2, (b) Cu-doped MoS_2 with sulfur vacancies (Cu@Vs-MoS_2), (c) V-doped Vs-MoS_2 (V@Vs-MoS_2), and (d) Sc-doped Vs-MoS_2 (Sc@Vs-MoS_2).

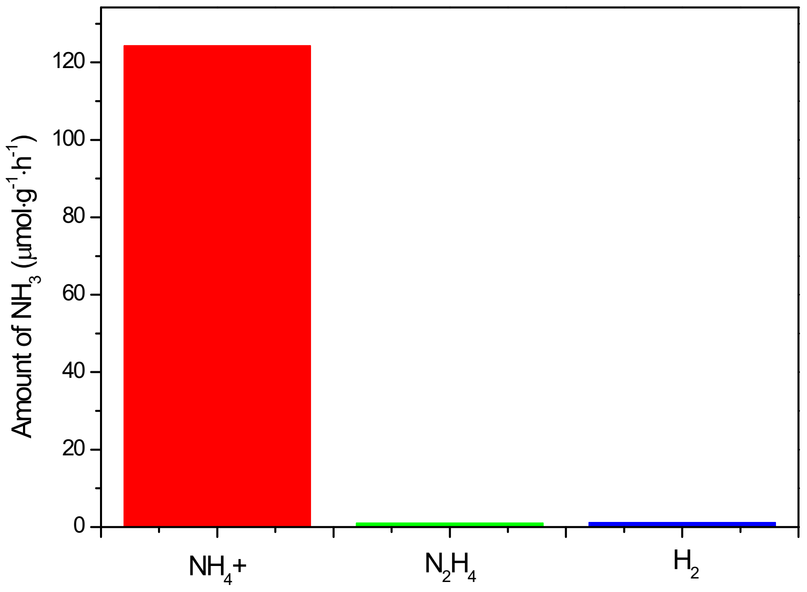

Figure S7. The test of nitrate (NO_3^-) and nitrite (NO_2^-) byproducts in the nitrogen reduction process.

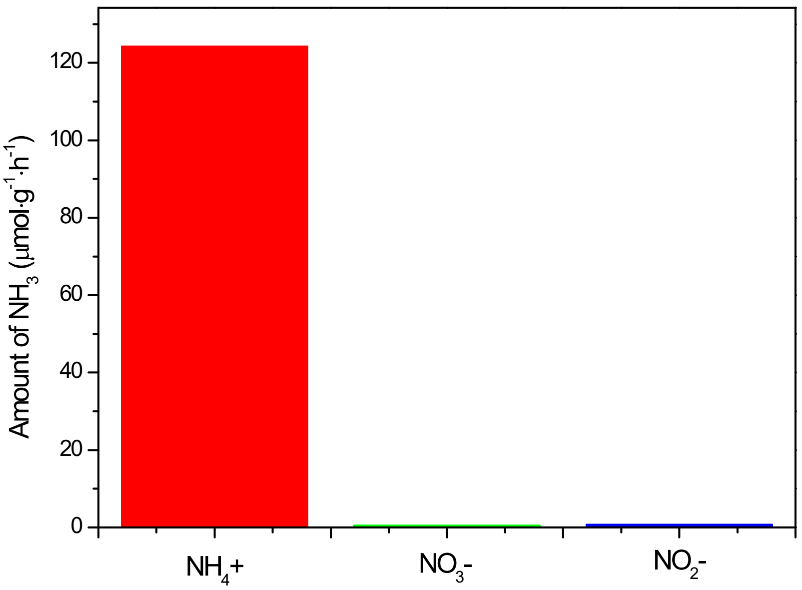

Figure S8. The test of hydrazine (N_2H_4) and hydrogen (H_2) byproducts in the nitrogen reduction process.

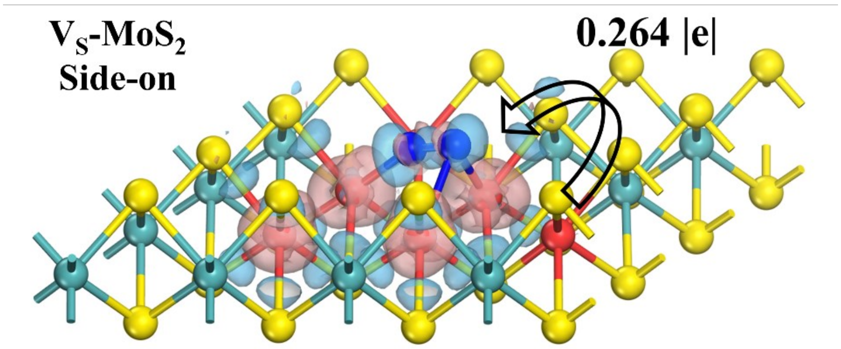

Figure S9. Deformation charge density diagrams of N_2 adsorbed on V_S–MoS_2 (blue color indicates charge accumulation, red color indicates charge departure, isovalue=0.060 e·Å^{-3}, arrows and numbers indicate the number of charges transferred).

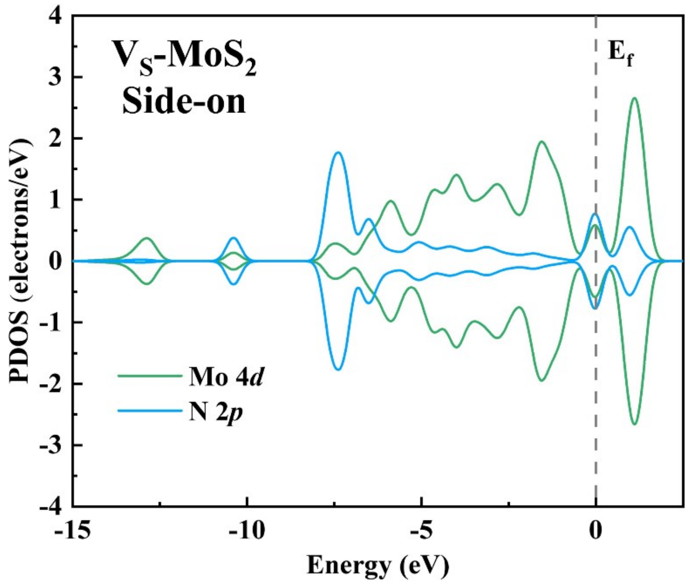

Figure S10. PDOS diagrams of N_2 adsorption on V_S−MoS_2.

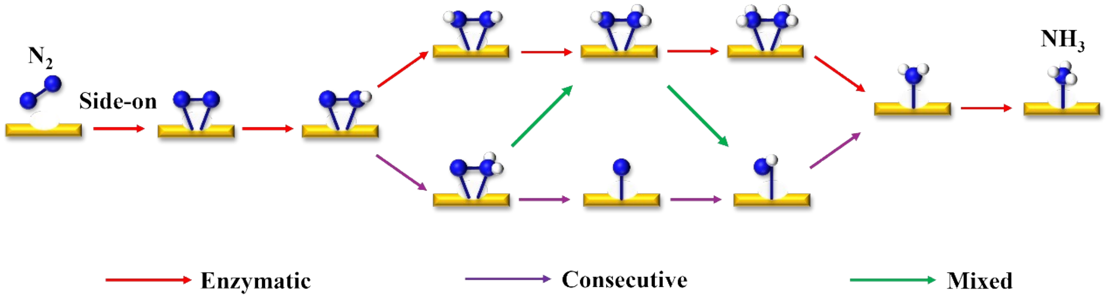

Figure S11. Mechanism diagram of N_2 reduction reaction to NH_3 under side-on adsorption (red is enzymatic path, purple is consecutive path, green is mixed path).

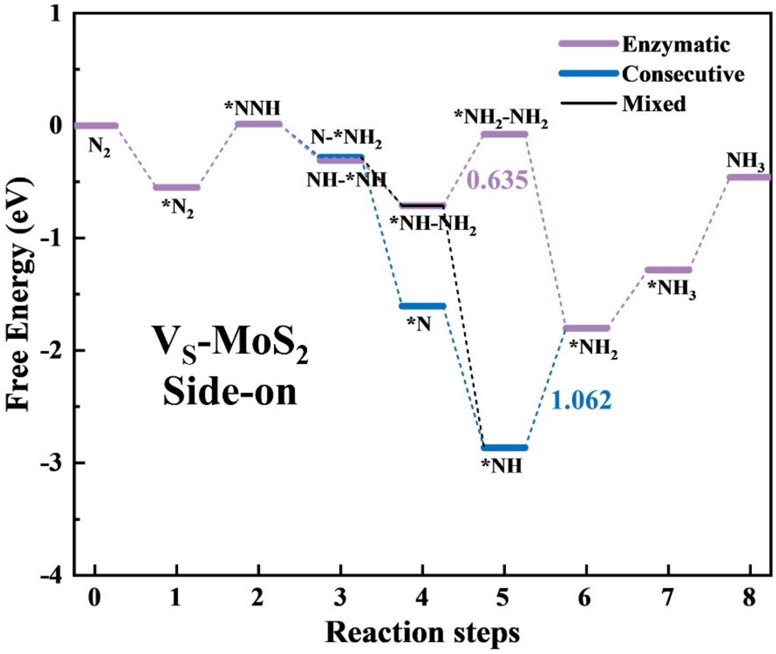

Figure S12. Free energy diagrams for reaction paths on V_S−MoS_2. Note: The numbers are the values of the potential decision step (PDS).

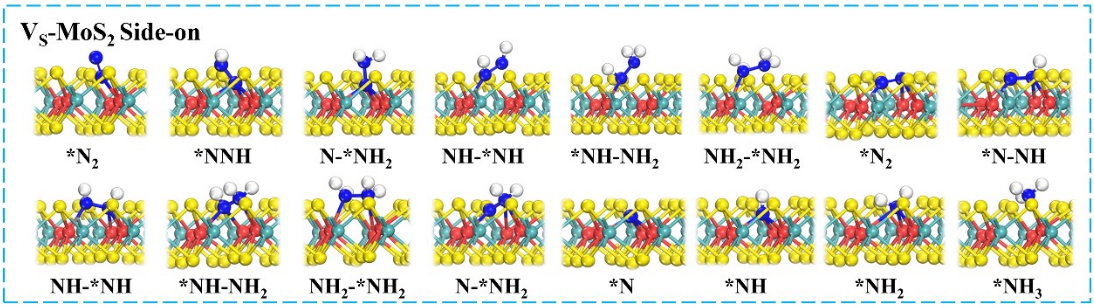

Figure S13. Optimized geometrical configurations of various reaction intermediates (N−*NH, N−*NH_2, NH−*NH, *NH, *NH_2, etc.) on V_S−MoS_2 structure.